arXiv:cond-mat/0505037v1 [cond-mat.str-el] 2 May 2005

Transport properties of strongly correlated electrons in quantum dots using a simple circuit model

G. B. Martins,[1,*] C. A. Büsser,[2,3] K. A. Al-Hassanieh,[2,3,4] E. V. Anda,[5] A. Moreo,[2,3] and E. Dagotto[2,3]

[1] *Department of Physics, Oakland University, Rochester, MI 48309*
[2] *Condensed Matter Sciences Division, Oak Ridge National Laboratory, Oak Ridge, Tennessee 37831*
[3] *Department of Physics and Astronomy, The University of Tennessee, Knoxville, Tennessee 37996*
[4] *National High Magnetic Field Laboratory and Department of Physics, Florida State University, Tallahassee, FL 32306*
[5] *Departamento de Física, Pontifícia Universidade Católica do Rio de Janeiro, 22453-900, Brazil*

Numerical calculations are shown to reproduce the main results of recent experiments involving nonlocal spin control in nanostructures (N. J. Craig *et al.*, Science **304**, 565 (2004)). In particular, the splitting of the zero-bias-peak discovered experimentally is clearly observed in our studies. To understand these results, a simple "circuit model" is introduced and shown to provide a good qualitative description of the experiments. The main idea is that the splitting originates in a Fano anti-resonance, which is caused by having one quantum dot side-connected in relation to the current's path. This scenario provides an explanation of Craig *et al.*'s results that is alternative to the RKKY proposal, which is here also addressed.

PACS numbers: 71.27.+a,73.23.Hk,73.63.Kv

The observation of the Kondo effect in a single quantum dot (QD)[1] and the subsequent theoretical and experimental studies of more complex structures, such as two QDs directly coupled through a tunable potential barrier[2], has provided impetus for the analysis of more elaborate systems. In a recent seminal work, Craig *et al.*[3] report on the possible laboratory realization of the two-impurity Kondo system. Two similar QDs are coupled through an open conducting central region (CR). A finite bias is applied to one of the QDs (QD1 from now on) as well as to the CR, while the other QD (QD2) is kept at constant gate potential. The differential conductance of QD1 is then measured for different charge states of QD2 and different values of its coupling to the CR. The main result was the suppression and splitting of the zero-bias-anomaly (ZBA) in QD1 by changing the occupancy of QD2 from even to odd number of electrons and by increasing its coupling to the CR. A Ruderman-Kittel-Kasuya-Yosida (RKKY) interaction between the QDs was suggested as an explanation for the observed effects[4]. The importance of Craig *et al.*'s experiments cannot be overstated: the possibility of performing nonlocal spin control in a system with two lateral QDs has potential applications in QD-based quantum computing[5].

In this Letter, numerical simulations in good agreement with the experiments are presented. The central conclusion of this work is that our computational data, and as a consequence the experimental results, can be explained using a very simple "circuit model", where one of the elements is a T-connected QD that has an intrinsic reduction of conductance with varying biases. This proposal is an alternative to the more standard RKKY ideas. Fig. 1a depicts the experimental set up used in the measurements of Craig *et al.*[3] with the labeling used in this Letter. Figure 1b is a schematic representation of the system, introducing two different tunneling parameters (hopping matrix elements t' and t'') and the Coulomb repulsion U in each QD (assumed the same for simplicity). To model this system, the Anderson impurity Hamiltonian is used for both QDs:

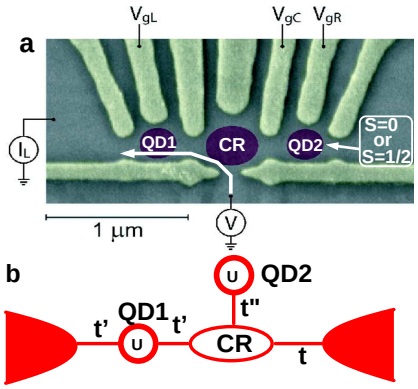


FIG. 1: (a) Experimental setup used in Ref. 3. (b) Illustration of the model studied in this Letter (see text for details).

$$H_{\rm d} = \sum_{i=1,2;\sigma} \left[U n_{i\sigma} n_{i\bar{\sigma}} + V_{\rm gi} n_{i\sigma} \right], \qquad (1)$$

where the first term represents the usual Coulomb repulsion between two electrons in the same QD, and the second term is the effect of the gate potential $V_{\rm gi}$ over each QD. QD1 is directly connected to the left lead and to the CR with hopping amplitude t', while QD2 is connected only to the CR (with hopping amplitude t''), which itself is connected to the right lead with hopping amplitude t (which is also the hopping amplitude in both leads, and our energy scale). In summary,

$$H_{\rm leads} = t \sum_{i\sigma} \left[c^\dagger_{li\sigma} c_{li+1\sigma} + c^\dagger_{ri\sigma} c_{ri+1\sigma} + \text{h.c.} \right], \qquad (2)$$

$$H_{12} = \sum_{\sigma} \Big[t' c^\dagger_{1\sigma} \left(c_{l0\sigma} + c_{\rm CR\sigma} \right) + t'' c^\dagger_{2\sigma} c_{\rm CR\sigma} +$$

$$tc^{\dagger}_{\mathrm{CR}\sigma}c_{r0\sigma} + \mathrm{h.c.}\Big], \qquad (3)$$

where $c^{\dagger}_{li\sigma}$ ($c^{\dagger}_{ri\sigma}$) creates an electron at site i with spin σ in the left (right) lead. The CR is composed of one tight-binding site[6], unless otherwise stated. Site '0' is the first site at the left (right) of QD1 (CR) in the left (right) lead. The total Hamiltonian is $H_{\mathrm{T}} = H_{\mathrm{d}} + H_{\mathrm{leads}} + H_{12}$. Note that for $V_{\mathrm{g1}} = V_{\mathrm{g2}} = -U/2$, the Hamiltonian is particle-hole symmetric. To calculate the conductance G, using the Keldysh formalism[7], a cluster containing the interacting dots and a few sites of the leads is solved exactly[8], the Green functions are calculated, and the leads are incorporated through a Dyson Equation embedding procedure. Details of the embedding have been extensively discussed before[9]. All the results shown were obtained for $U = 0.5$, $t' = 0.2$, zero-bias, and zero temperature.

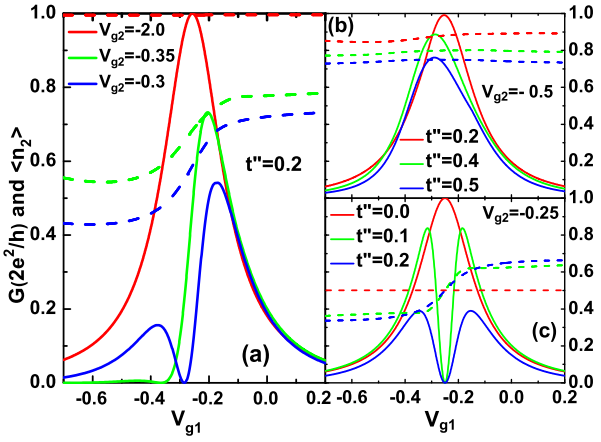


FIG. 2: (a) Variation of G with V_{g1} in QD1 (solid curves) and variation of $\langle n_2\rangle$ (occupancy of QD2 per spin orientation - dashed curves) for $t'' = 0.2$ and three different values of V_{g2}. For $V_{\mathrm{g2}} = -2.0$ (red), QD2 is occupied by 2 electrons ($\langle n_2\rangle = 1$) for any V_{g1} and the conductance through QD1 is essentially the same as if QD2 was not present. For higher values of V_{g2}, the average value of $\langle n_2\rangle$ decreases and becomes dependent on V_{g1} (decreasing for lower values of V_{g1}). This is accompanied by a suppression of the ZBA (for -0.35 (green)) and also by a splitting of the ZBA (for $V_{\mathrm{g2}} = -0.3$ (blue)). (b) Variation of G and $\langle n_2\rangle$ with t'' (0.2, 0.4, 0.5) at a fixed value of $V_{\mathrm{g2}} = -0.5$. As the value of t'' increases, the average value of $\langle n_2\rangle$ decreases and this is again accompanied by a suppression of the ZBA. (c) Same as in (b), but now for $V_{\mathrm{g2}} = -0.25$ (particle-hole symmetric point) and $t'' = 0.0$, 0.1, and 0.2. Note that G vanishes at $V_{\mathrm{g1}} = -0.25$, where $\langle n_2\rangle = 0.5$, for all finite values of t''.

In Fig. 2, results for the conductance across QD1 (solid curves) and for the occupancy per spin orientation $\langle n_2\rangle$ of QD2 (dashed curves) are presented. In Fig. 2a, $t'' = 0.2$ and V_{g2} varies from -2.0 to -0.3. For $V_{\mathrm{g2}} = -2.0$ (red), QD2 is occupied by two electrons ($\langle n_2\rangle = 1$) and the conductance of QD1 displays the characteristic Kondo behavior reported before[10]. For $V_{\mathrm{g2}} = -0.35$ (green) the average value of $\langle n_2\rangle$ decreases to ≈ 0.7 (≈ 1.4 electrons in QD2) and $\langle n_2\rangle$ now depends on V_{g1}. In addition, G decreases in comparison to the result obtained for $V_{\mathrm{g2}} = -2.0$. Then, these numerical results are qualitatively in agreement with the experimental results shown in Fig. 2 of Craig *et al.*[3], namely, by decreasing the occupancy of QD2, from even to odd number of electrons, the ZBA in QD1 is suppressed. As V_{g2} is further increased (-0.3 (blue)) a *qualitative* change occurs: For values of V_{g1} where $\langle n_2\rangle \approx 0.5$ (QD2 singly occupied), the conductance of QD1 vanishes and therefore there is a narrow dip in G. This splitting of the ZBA is remarkably similar to that observed in Fig. 3A of the experimental results[3]. For finite-temperature calculations, the dip in G will not reach zero, resembling even better the experiments[11].

To further test the similarities between simulations and experiments, in Figs. 2b and 2c results for G and $\langle n_2\rangle$ are shown for fixed V_{g2} and different t'' values. In Fig. 2b, where $V_{\mathrm{g2}} = -0.5$, as t'' increases from 0.2 to 0.5 there is only a slight decrease of G. This is accompanied by a slight decrease in the average value of $\langle n_2\rangle$, from ≈ 0.9 to ≈ 0.7. A more dramatic change is obtained in Fig. 2c, where $V_{\mathrm{g2}} = -0.25$, and t'' varies from 0.0 to 0.2. By increasing t'' from 0.0 (red curves) to 0.1 (green), the ZBA is now split in two and $\langle n_2\rangle$ acquires a dependence on V_{g1}. As t'' further increases (0.2 (blue)), the dip becomes wider, the two side-peaks decrease and G still vanishes for $\langle n_2\rangle = 0.5$ (one electron in QD2). Our calculations show that, if $\langle n_2\rangle$ varies around 0.5, the dip in G is present for all finite values of t'', with a width proportional to t''. Comparing the results in Figs. 3A and 3B of Craig *et al.*[3] with Figs. 2c and 2b in this Letter, respectively, one notices a striking similarity: The splitting of the ZBA observed in the experimental results (their Fig. 3A), when the number of electrons in the control QD is odd and the coupling to the central region is increased, is very similar to the dip in G for all finite-t'' curves in Fig. 2c (as mentioned above, at finite temperatures, one expects that the dip in G will not reach zero). When the occupancy of QD2 is even (Fig. 3B in the experimental results[3] and Fig. 2b in this Letter), the G dependence on t'' is much less significant and the splitting of the ZBA does not occur.

What is the origin of these results? Below, it will be argued that a qualitative description of the results can be achieved by analyzing the two quantum dots through a so-called 'circuit model'. This model starts with the conductance of each QD calculated separately, as independent elements of a circuit, and then the conductance of the 'complete circuit' is obtained by combining the conductances of the two elements connected in series. Fig. 3 describes schematically the steps involved in this approach. In Fig. 3a, the complete system formed by QD1 and QD2 (shown in Fig. 1b) is divided into two components. QD1 is modeled as a QD connected directly to left (L) and right (R) leads, while QD2 is modeled as a side-connected QD[12]. Fig. 3b shows the respective conductances and occupancies for each independent element vs. gate voltage, and Fig. 3c represents the scattering processes (represented by transmission and reflection ampli-

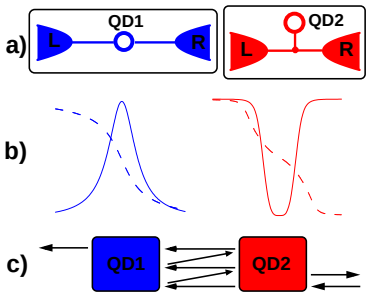


FIG. 3: Schematic representation of the main ideas behind the "circuit model". In (a), the system represented in Fig. 1b is divided into its constituent elements: QD1 is modeled as a QD connected in series with the leads and QD2 is modeled as a side-connected QD. The curves in (b) represent the conductance and occupancy of each separate circuit element vs. the applied gate potential. (c) Schematic representation of how the two individual elements are connected to form the final 'circuit': Incident and reflected wave amplitudes are represented in the right side of QD2 by black arrows. A transmitted wave through QD2 undergoes multiple reflections between the two quantum dots until it is finally transmitted past QD1. The superposition of all these processes results in the final conductance for the 'circuit'.

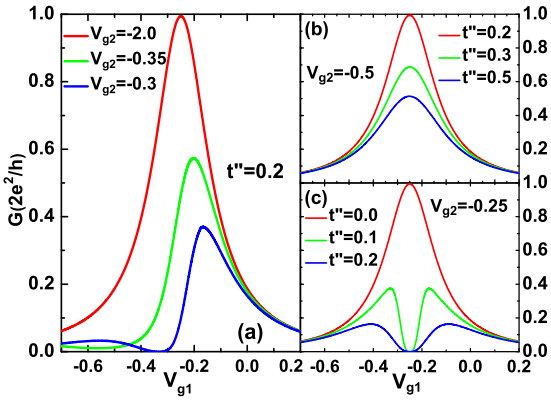


FIG. 4: Same as in Fig. 2, but now using the 'circuit model' for the calculations.

tudes) that an electron undergoes while moving through the complete 'circuit'. The superposition of all these processes leads to the total transmittance (proportional to the conductance) for the circuit model. This can be calculated in two ways: coherently or incoherently[13]. Since there is no qualitative difference between them, and in order to keep the simplicity of the model, we present the incoherent results. The equation which provides the final transmittance for the processes depicted in Fig. 3c is

$$T = \frac{T_1 T_2}{1 - R_1 R_2}, \tag{4}$$

where the transmittances T_1 and T_2 are proportional to the conductances for QD1 and QD2, as depicted in Fig. 3b, and $R_{1(2)} = 1 - T_{1(2)}$ are the reflectances. To calculate T, one needs to establish how T_2 depends on V_{g1}. The natural way to do that is to use the dependence of $\langle n_2 \rangle$ on V_{g1}, as depicted in Fig. 2, and then use the relation between conductance and occupancy, as shown in the red curves in Fig. 3b. In other words, the functional relation can be expressed as $T_2 = T_2(\langle n_2 \rangle(V_{g1}))$. It is not surprising that in a strongly correlated system like the one being analyzed here, the variation of the gate potential of QD1 will influence the charge occupancy of QD2, and in turn this will influence the conductance through QD1.

In Fig. 4, conductance results using Eq.(4) are shown for the same parameters as in Fig. 2. Although the quantitative agreement varies, there is good overall qualitative agreement. All the trends are correctly reproduced and some of the details are quite similar, such as for example the asymmetric shape of the curves at higher values of V_{g2} (-0.35 and -0.3) in Fig. 4a. It is important to notice that there are *no* adjustable parameters in the circuit model here presented. The only input necessary is $\langle n_2 \rangle$ vs. V_{g1}, which is obtained through a calculation for the complete system (values displayed for $\langle n_2 \rangle$ in Fig. 2). The success of the circuit model implies that the dip in G arises from the Fano anti-resonance which cancels the conductance of QD2 (red solid curve in Fig. 3b). The Fano anti-resonance can be seen as a destructive interference process between two different trajectories an electron can take on its way to QD1: it can cross the CR without passing through QD2; or it can visit QD2, return to the CR and then proceed to QD1[12].

The similarities between the experimental results and our simulations suggest that our model and numerical technique have captured the essential physics of the experiments. However, these same experiments have also been explained using RKKY ideas[4]. Can our numerical results be also understood in this alternative context? To try to answer this question, several calculations were performed with different parameter values and number of sites in the CR[14]. In Fig. 5a, results for spin correlations between QD1 and QD2 (denoted $\mathbf{S_1} \cdot \mathbf{S_2}$) are presented for the same parameters used in Fig. 2c. At $t'' = 0.0$ (red curve) QD1 and QD2 are uncorrelated as expected. As t'' increases to 0.1 (green), and then 0.2 (blue), it is observed that in the region where G reaches its maximum value (see Fig. 2c), $\mathbf{S_1} \cdot \mathbf{S_2}$ also assumes a maximum value and it is positive (ferromagnetic (FM)). For $t'' > 0.2$ (not shown), $\mathbf{S_1} \cdot \mathbf{S_2}$ saturates and starts decreasing. The maximum of $\mathbf{S_1} \cdot \mathbf{S_2}$, for all values of t'', decreases even further as the size of the central region increases (the results in Fig. 5a are for a CR with just one site). In addition, the sign of $\mathbf{S_1} \cdot \mathbf{S_2}$ alternates as the size of the CR increases and the QDs move farther apart from each other. In Fig. 5b, results for the spin correlation between QD1 and its neighboring site in the CR (denoted $\mathbf{S_1} \cdot \mathbf{S_c}$) is shown for the same parameters as in Fig. 5a. $\mathbf{S_1} \cdot \mathbf{S_c}$ is a rough measure of the Kondo correlation in QD1, having a direct connection with the ZBA in Fig. 2c. Indeed, for $t'' = 0.0$ (red) when G reaches the unitary limit, a robust antiferromagnetic (AF) cor-

relation develops between QD1 and its neighboring site in the CR. For $t'' = 0.1$ (green), despite the narrow dip in G, the side-peaks are still close to the unitary limit (see Fig. 2c) and $\mathbf{S_1} \cdot \mathbf{S_c}$ is still strongly AF. However, for $t'' = 0.2$ (blue), both G and $\mathbf{S_1} \cdot \mathbf{S_c}$ are strongly suppressed, in qualitative agreement with a suppressed ZBA due to a weakened Kondo resonance.

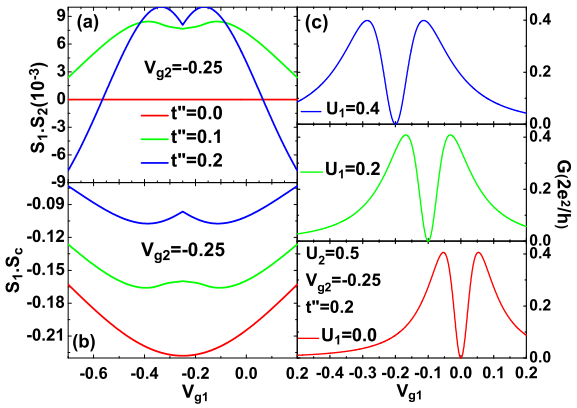


FIG. 5: (a) Spin correlation $\mathbf{S_1} \cdot \mathbf{S_2}$ between QD1 and QD2 for the same parameters as in Fig. 2c. For $t'' = 0.0$ (red curve), the two QDs are uncorrelated ($\mathbf{S_1} \cdot \mathbf{S_2} = 0$). For finite t'' (0.1 (green) and 0.2 (blue)), $\mathbf{S_1} \cdot \mathbf{S_2}$ is FM and reaches its maximum value in the region where G is maximum. (b) Kondo correlations $\mathbf{S_1} \cdot \mathbf{S_c}$ between QD1 and the central site for the same parameters as in (a). All values are AF and they decrease in amplitude as t'' increases, underscoring the decrease of the Kondo effect as the FM correlation between QD1 and QD2 increases (compare with (a)). (c) Variation of G as U_1 (Hubbard interaction in QD1) assumes the values 0.4, 0.2 and 0.0. Note that the dip in G becomes slightly narrower as U_1 decreases, however it does not disappear.

The results thus far seem to indicate that the CR could be mediating a long range coupling between QD1 and QD2, with the characteristics of an RKKY interaction. However, the magnitude of the maximum value of $\mathbf{S_1} \cdot \mathbf{S_2}$ (see scale in Figs. 5a-b) is too small to account for all the effects observed in the conductance in Fig. 2c. One possible way of increasing $\mathbf{S_1} \cdot \mathbf{S_2}$ is by coupling QD1 more strongly to the CR than to the left lead. This was exactly the setup chosen in Ref. 3, where those authors performed the measurements with asymmetric couplings to the left ($\Gamma_{\rm L}$) and right ($\Gamma_{\rm CR}$) sides of QD1. In fact, the voltages applied to the gates in Fig. 1a were such that $\Gamma_{\rm CR} \gg \Gamma_{\rm L}$. In our model, this is equivalent to having an asymmetric t', with $t'_{\rm CR} \gg t'_{\rm L}$. An analysis of the results in this asymmetric regime indicates that the correlation between QD1 and QD2 does indeed increase. However, if one performs the calculations with the sites in the CR at a filling lower than one electron per site (half-filling), it is observed that $\mathbf{S_1} \cdot \mathbf{S_2}$ is gradually suppressed as the electron filling falls to a more appropriate level to simulate the two-dimensional electron gas in the CR. Although one can argue that some of the dependence of the conductance of QD1 on the charge state of QD2 seen in Fig. 2 is associated to the correlations between the two dots, it is apparent that other effects are also present. This is dramatically exemplified by the fact that the cancellation of G presented in Fig. 2c occurs for *any* finite value of t'', and of course for $t'' \approx 0$, one finds that $\mathbf{S_1} \cdot \mathbf{S_2} \approx 0$. The fact that the dip seen in the conductance in Fig. 2c is not dominantly caused by correlations between the dots can be made more clear by checking the results for the conductance as U_1 (Hubbard interaction in QD1) is reduced to zero. In Fig. 5c, results for G are shown for 3 different values of U_1, for the same parameters as for the blue curve in Fig. 2c. As U_1 decreases from 0.4 (blue) to 0.2 (green), and then to 0.0 (red), the dip in the conductance remains, only becoming narrower, indicating that its origin is not associated with many-body interactions, but more likely with cancellations typical of T-geometries[12] that occur even in the non-interacting limit.

In summary, the numerical results qualitatively reproduce the main aspects of important recent experiments[3] involving nonlocal spin control in nanostructures. The main result is that the splitting observed in the ZBA is caused by a cancellation in the conductance due to a destructive interference. This so-called Fano anti-resonance has its origin in one of the dots being side-connected to the current's path. A simple 'circuit model' qualitatively reproduces the experiments and offers an alternative to a purely RKKY interpretation of the results, underscoring that a laboratory realization of the two-impurity Kondo system should avoid any geometry susceptible to a Fano anti-resonance.

C.B., K. A., A. M., and E. D. are supported by NSF grant DMR 0454504. G. M. by an OU internal grant.

* corresponding author: martins@oakland.edu

[1] D. Goldhaber-Gordon *et al.*, Nature **391**, 156 (1998).
[2] W. G. van der Wiel *et al.* Rev. Mod. Phys. **75**, 1 (2003).
[3] N. J. Craig *et al.*, Science **304**, 565 (2004).
[4] L. I. Glazman *et al.*, Science **304**, 524 (2004); P. Simon *et al.*, Phys. Rev. Lett. **94**, 086602 (2005); M. G. Vavilov *et al.*, Phys. Rev. Lett. **94**, 086805 (2005).
[5] D. Loss *et al.*, Phys. Rev. A **57**, 120 (1998).
[6] Calculations for a CR with a larger number of sites did not present any qualitatively new results.
[7] Y. Meir *et al.*, Phys. Rev. Lett. **66**, 3048 (1991).
[8] Results shown include one site on each side. Calculations with more sites were done, but no significative size-effects were observed.
[9] See V. Ferrari *et al.* Phys. Rev. Lett. **82**, 5088 (1999).
[10] Removing QD2 results in essentially the same conductance as the one for $V_{g2} = -2.0$.
[11] R. Franco *et al.*, Phys. Rev. B **67**, 155301 (2003).
[12] M. Sato *et al.*, cond-mat/0410062.
[13] S. Datta, *Electronic Transport in Mesoscopic Systems*,

Cambridge University Press (1995).
[14] A full discussion of results will be presented in G. B. Martins *et al.*, in preparation.